

Ionospheric Research
ARO Grant DA-ARO-D-31-124-G659
Scientific Report
on
"D-Region Probe Theory and Experiment"

by

Ta-jin Kuo


November 30, 1966

Scientific Report No. 285

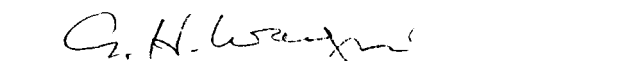
"The research reported in this document has been supported by the Army Research Office-Durham under Grant DA-ARO-D-31-124-G659 and, in part, by the National Aeronautics and Space Administration under Grant NsG-134-61. "

Submitted by:


L. C. Hale, Assistant Professor of
Electrical Engineering


J. S. Nisbet, Associate Professor of
Electrical Engineering

Approved by:


A. H. Waynick, Director, Ionosphere
Research Laboratory

Ionosphere Research Laboratory
The Pennsylvania State University
College of Engineering
Department of Electrical Engineering

Table of Contents

	Page
Abstract	i
I. Introduction	1
II. Weak Shock Effects and the Chemistry of the Lower D Region	2
III. Blunt Subsonic Probe Theory and First Order Corrections .	4
IV. Experiments	10
V. Conclusions	15
References	16
Acknowledgments	17

ABSTRACT

A chemistry model for the lower D region at nighttime is discussed, which is confirmed by rocket experiments. The first approximate theory of subsonic blunt probes used in measuring ionic conductivities and densities is presented, which is accurate to within 10%. It was discovered through measurements that the negative conductivity exceeds the positive conductivity by some 25%.

I Introduction

This report discusses the previous three papers by Hoult ⁽¹⁾, ⁽²⁾, ⁽³⁾ on the theoretical investigation of the physics of the possible probes used in the direct D region measurements and two papers by Hale et al. ⁽⁴⁾, ⁽⁵⁾ on the blunt subsonic probe system, the electronics, the measurements and the conclusions of experiments.

It is desirable to have a probe system which is theoretically simple, and is not subject to too stringent a restriction on its operation condition. Supersonic probes drastically affect the composition of the medium through shock waves which are yaw-dependent. Hence supersonic probes are sensitive to the variation of the angle of attack. Probes which are sensitive to the variation of the angle of attack, including the Gerdien condenser, are not considered in this report. The analysis for the weak shock wave effects on the chemistry of the lower D region are discussed in Section II.

The blunt subsonic probe, which is hung under a large parachute to reduce it to low subsonic speeds, is relatively simple, insensitive to the swing and inexpensive. Section III establishes the first approximate relation between measured current, probe voltage and the environment number densities of the charged particles for a blunt subsonic probe and provides an outline of a method of systematic improvement and estimation of the accuracy of the first approximation.

The actual measurements and findings of rocket experiments using blunt subsonic probes are described in Section IV. For a more accurate measurement of conductivity, a sweep potential was applied instead of a fixed potential, with the sweep frequency of about 10^{-1} sec. This frequency is so low that the operation of the probe can be described by a quasi-static theory.

II Weak Shock Effects and the Chemistry of the Lower D Region

Densities of the principal constituents of the atmosphere and of the charged particles are summarized by Hoult⁽¹⁾. The mean free path of neutrals is 10^{-2} cm at 50 km, and 10 cm at 90 km. Hence for a sounding rocket of 30 cm diameter traversing the lower part of D region with a Mach* 2 speed, a weak oblique shock will be formed at its nose cone up to 80km.

Since the chemical reactions across and after the weak shock are not in equilibrium⁽¹⁾, a more detailed study with finite rate chemistry is in order. The rate equations for the various charged particles⁽⁶⁾ are:

$$\begin{aligned}\frac{dN^e}{dt} &= q + \rho N^- + kNN^- - aN^2N^e - \alpha_d N^e N^+ \\ \frac{dN^-}{dt} &= aN^2N^e - \rho N^- - kNN^- - \alpha_i N^- N^+ \\ N^+ &= N^- + N^e\end{aligned}\tag{1}$$

Here N^+ , N^- , N^e , N are densities of the positive ions, negative ions, electrons and neutrals respectively. q is the rate of production of electrons and positive ions by primary ionization. ρ is the photodetachment rate coefficient. k is the collisional detachment coefficient. a is the three-body attachment coefficient. α_d , the dissociative recombination coefficient. α_i , the mutual neutralization coefficient. The details of these individual reactions as well as the magnitudes of the rate coefficients are mostly given by Hoult⁽¹⁾. No distinction is made here between nitrogen and oxygen in view of the more important uncertainties in reaction rates and in effects of impurities.

At night launches, photodetachment is negligible; the primary ionization q comes from the galactic cosmic rays alone. For lower altitudes, say below 65 km, dissociative recombination is also unimportant due to the low electron density. By neglecting collisional detachment through actual numerical comparison, Hale⁽⁵⁾ arrived at the following simplified rate equations for nighttime:

* Mach number = $M = U/a$, U = probe velocity, a = local speed of sound.

$$\begin{aligned}\frac{dN^e}{dt} &= q - aN^2N^e \\ \frac{dN^-}{dt} &= aN^2N^e - \alpha_1 N^- N^+ \\ N^+ &= N^- + N^e \approx N^-\end{aligned}\tag{2}$$

From this model, Hale obtained the equilibrium distribution for ion densities at night

$$N^+ \approx N^- \approx \sqrt{\frac{q}{\alpha_1}} \propto \sqrt{N}\tag{3}$$

By analyzing reactions involving the neutrals and (1), Hoult⁽¹⁾ concluded the N and N^+ species are frozen across the shock, i. e. their percentage changes are equal to the density jump across the shock. For negative ions, taking into account the density jump caused by the weak shock, we have, from (2)

$$\frac{dN^-}{dt} = N^- \frac{d \ln \rho}{dt} + aN^2N^e - \alpha_1 N^- N^+\tag{4}$$

Retaining only the fastest reaction, viz. the three-body attachment process, we eventually obtain the relative change of N^- across and after the weak shock for nighttime⁽¹⁾:

$$\begin{aligned}\frac{\Delta N^-}{N^-(\infty)} &= \frac{\Delta \rho}{\rho} + \frac{N^2(\infty)}{N^{+2}(\infty)} \left(\frac{N^+(\infty)}{N^-(\infty)} - 1 \right) \left(\frac{\Delta T}{T} + \frac{3\Delta \rho}{\rho} \right) \\ &\quad \left(1 - \exp - \frac{aN^{+2}(\infty)x}{u} \right)\end{aligned}\tag{5}$$

with the boundary condition $\left. \frac{\Delta N^-}{N^-(\infty)} \right|_{x=0} = \frac{\Delta \rho}{\rho}$, in which ρ and T are the density and temperature of the gas medium. x is the distance downstream from the shock, and u is the velocity behind the shock. For a wedge of 5° half-angle at Mach 2, $\Delta \rho / \rho = 0.50$. Ignoring the shock gives a 50% error in percentage composition just behind the shock. At 50 km, 10 centimeters behind the shock, the second term in (5) adds 12%. With the exponential decrease of $N^2(\infty)$ with increasing altitude, the second term is negligible

above 70 km. The change in electrons through weak shocks can be obtained from charge balance.

From the above discussions, a model of positive ion density being proportional to the square root of the local neutrals is proposed, which will be checked with the experimental data in Section IV. It is also shown that the flow through the shock and downstream is essentially frozen. Since in its actual descent, the nose cone constantly changes its angle of attack, thus changing $\Delta\rho/\rho$, the data obtained will be sensitive to the angle of attack. Thus we are led to a discussion of subsonic probes.

Section III Blunt Subsonic Probe Theory and First Order Corrections

This section is essentially a summary of two papers by Hoult⁽²⁾, Hoult and Kuo⁽³⁾. For more details, in particular the governing equations and the formal deduction, please refer to these papers.

A typical subsonic probe dimension is 10 cm; velocity, 100 m/sec; voltage, 5V. This gives the Mach number of about 3/10 and the nondimensionalized voltage $\phi_w (= \frac{eV}{\kappa T_\infty}$, κ = Boltzmann's constant, T_∞ = environment temperature, e = electron charge, V = probe voltage) about 2×10^2 . The ratio of the Debye length to body dimension is 1 at 50 km, about 1/3 at 80 km. The Reynolds number $Re (= UL/\nu$, U = free stream velocity, L = probe dimension, ν = kinematic viscosity) varies from 5×10^2 at 50 km to 10 at 80 km. Hence there is a laminar boundary layer over the blunt probe, and there is no boundary layer separation. The diffusion Reynolds number $Rd (= \frac{UL}{D}$, D = binary diffusion coefficient for positive or negative ions) is 10^3 at 50 km and 10 at 80 km. It is shown in reference 2 that the concept of mobility is appropriate up to 70 km.

From the characteristics given the following realistic assumptions are made: (1) The Mach number is small. This allows the use of incompressible flow as a first approximation. (2) The temperature difference

between the probe and the environment is small, allowing adiabatic flow as a first approximation. (3) The charged particle density is so low that α , the ratio of Debye length to probe dimension, is of order one, and the thickness of the diffusion layer, $\frac{L}{\phi_w}$, is small compared to L yet is greater than the mean free path. This insures that Laplace's equation is the first approximation to Poisson's equation, and that the motion of the ions is describable by a continuum theory with an appropriate mobility. This sets an upper limit of the rigorous application of theory to altitudes below 70 km and a probe voltage of 2/10 volts, for a probe dimension of 10 cm. The low concentration of charged particles also insures that the fluid mechanical motion can be uncoupled from the electric field. (4) Re is such a size that $Re^{-\frac{1}{2}}$, the nondimensional boundary layer thickness, is greater by an order of magnitude than $1/\phi_w$, the nondimensional diffusion layer thickness, as is illustrated in fig. 1. This gives 40 km as the lower limit to the theory, for a probe of 10 cm and a probe voltage of 10 volts.

Under these assumptions, the first approximation to the problem is a nonreacting, incompressible, adiabatic flow towards a highly charged collector, the electric field around it being governed by Laplace's equation. With the fluid mechanics and electrostatics uncoupled and presumably solved in advance, the problem that remains is to obtain the number density profiles about the collector from the species conservation equations.

For steady state processes, species conservation requires that the convection of a certain species through a control volume be equal to its production rate inside that volume. That species convection comes from three sources: (1) mobility, due to the presence of the probe potential; (2) diffusivity, due to the concentration gradient associated with the assumption that the collector surface be perfectly absorbing; (3) fluid mechanics,

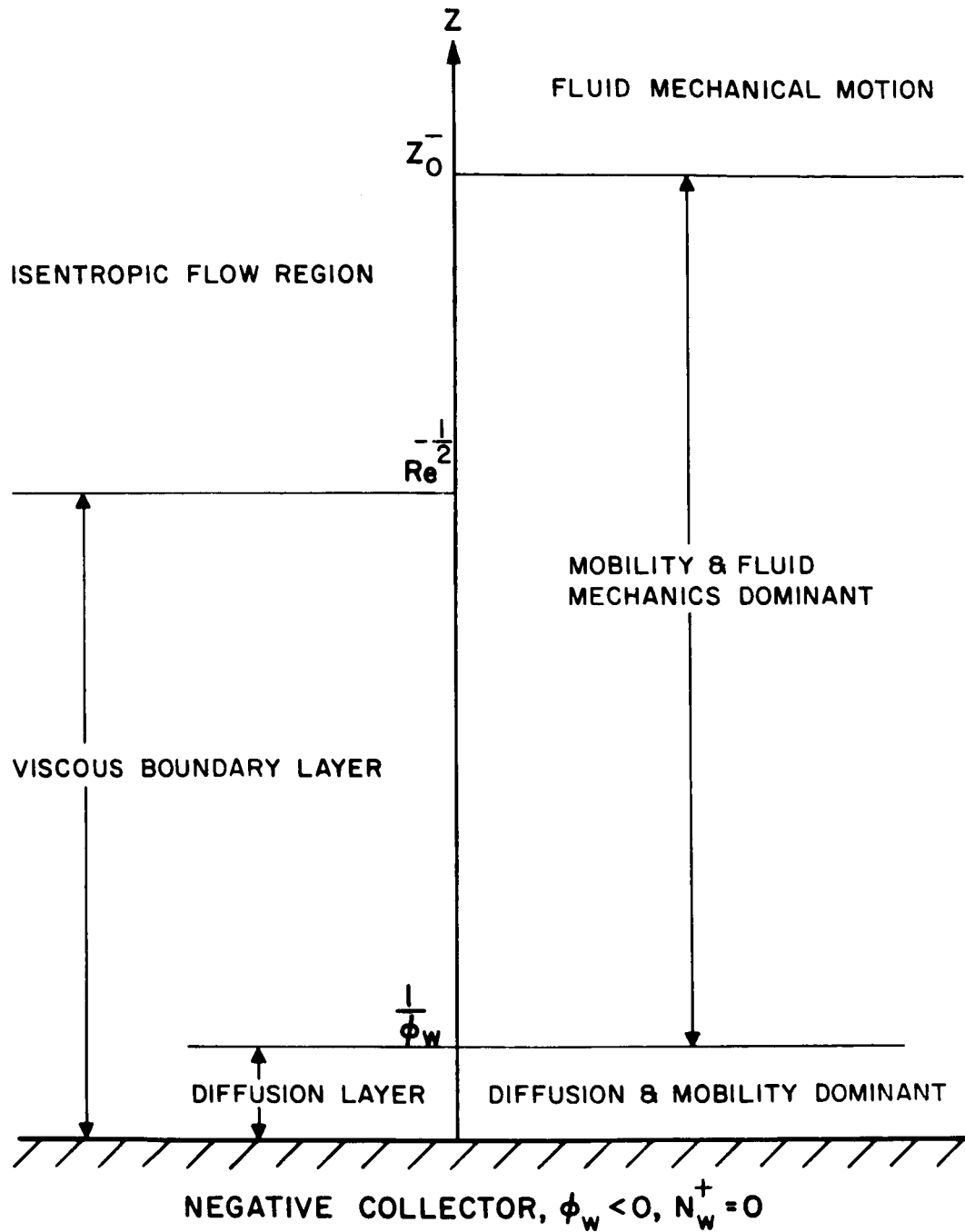


FIGURE 1. SCHEMATIC DIAGRAM FOR N^+ SPECIES TOWARDS A HIGHLY NEGATIVE COLLECTOR. z_0^- IS THE STAND-OFF DISTANCE FOR N^-

due to the entrainment of that species in the neutrals, viz. its being carried along by the bulk flow. For the species being collected, e.g., the positive ions in the case of a negative collector, the diffusion process of N^+ takes place essentially within the diffusion layer, outside of which diffusivity becomes negligible compared to fluid mechanical motion and mobility. Whereas inside the diffusion layer, the fluid mechanical motion is negligible. This is because the bulk flow velocity at the wall is zero (due to viscosity), and that the diffusion layer is assumed to be an order of magnitude thinner than the viscous boundary layer. The simplification brought forth by this physical argument is illustrated in fig. 1.

The simplified equation valid inside the diffusion layer obtained by dropping the fluid mechanical convection term is called diffusion layer equation. The first approximation to the diffusion layer problem was solved by Hoult⁽²⁾, giving the number density profiles and the current collected by the probe. Here an alternative physical argument (due to Hale) leading to the same result is presented as follows:

The stagnant portion of the medium covering the collector extends to a distance somewhat beyond the diffusion layer (fig. 1). At the edge of the diffusion layer, mobility is the predominant mechanism governing the motion of the species being collected. Moreover, in view of the thinness of the diffusion layer, the current towards the collector is essentially a one-dimensional flow with constant intensity in the diffusion region. Hence the positive ion current to a negative collector is equal to the current across the surface at the edge of the diffusion layer with the same area as the collector, the electric field there being E_w , the ion density there being N_w^+ . Thus

$$dI_o^+ = -eN_{\infty}^+ \mu_{\infty}^+ E_w ds \quad (6)$$

where μ_{∞}^+ is the environmental positive ion mobility. Noting that the conductivity of species i , $\sigma^i = eN_{\mu}^i$, we can yet obtain another representation of the current

$$dI_o^+ = -\sigma_{\infty}^+ E_w ds \quad (7)$$

In a similar vein, the electron and negative ion currents to a positively charged surface ds is

$$dI_o^- = \sigma_{\infty}^- E_w ds + \sigma_{\infty}^e E_w ds \quad (8)$$

In the next section, variant forms of (7) and (8) will be introduced which are more wieldy in dealing with the experiments.

The above first approximate relations (6), (7), (8) show that the current measured is proportional to the probe voltage and the electric field at the collector surface. Furthermore, in the first approximation, since the diffusion layer equation as well as its boundary conditions do not involve fluid mechanics of the bulk flow, conclusions (6), (7), (8) are insensitive to the change of angle of attack.

It is important to examine the accuracy of (6), (7), (8) for practical applications from these two aspects. First, is the current contribution from negative ions and electrons to a negative probe negligible compared to that from positive ions as given by (6), (7)? For a specific geometry of a small negatively charged collector ($r \ll L$) placed at the stagnation point, the answer is affirmative. That implies the current actually measured can be regarded as the one from positive ions alone. Reference 2 gave the order of magnitude estimates of the current contribution from N^- and N^e , thereby showing they are indeed negligible. Reference 2 also introduced the important concept of stand-off distance. For λ (the ratio of free

stream negative ion density to electron density) greater than order one, the stand-off distance of negative ions, z_0^- , is particularly important. For a region beyond z_0^- , fluid mechanical motion dominates mobility effects not only in the case of negative ions, but also in the case of positive ions, since the electric field of the negative collector is then virtually shielded off beyond $z_0^{-(3)}$. Similar order-of-magnitude conclusions also hold for a positive probe. Second, is the first approximation to the problem accurate enough without further corrections? For the same specific geometry, the answer is again affirmative⁽³⁾. Therefore, within sufficient accuracy, we can regard (8) as a current-wall electric field relation for a positive probe which is insensitive to the change of angle of attack. Parallel conclusions can be drawn for (6), (7).

The four assumptions discussed earlier are associated with four corrections of the problem, viz. compressibility, heat transfer, sheath effect and finite diffusion layer thickness corrections, plus a fifth one associated with chemical reactions. We want to outline here the general scheme for tackling the two most important corrections: heat transfer and compressibility effects, of orders ϵ ($=(\Gamma_w - T_s)/T_\infty$, T_w = wall temperature, T_s = adiabatic temperature) and M^2 respectively. The approach to these two effects are identical in principle, only differing in details. Here the discussion is expediently restricted to the correction on the positive ion current towards a small negatively charged collector placed at the stagnation point.

First, from $dI_o^+ = eD \frac{\partial N^+}{\partial Z} \Big|_w ds$, the ϵ - order (or M^2) correction comes in through its affecting the diffusivity at the wall and the number density gradient at the wall. To account for the change of diffusivity is a

straightforward computation. As to the change of number density gradient at the wall, it is convenient to obtain two simplified versions of the ϵ -order (or M^2) governing equation, one is the diffusion layer equation, the other is the one which is valid outside the diffusion layer, involving only mobility and fluid mechanical convection (fig. 1). The latter is a first order differential equation with the boundary condition at infinity already specified. The solution to the latter problem gives the ϵ -order (or M^2) positive ion profile outside the diffusion layer. The ϵ -order positive ion density at the edge of the diffusion layer supplies the second boundary condition (the first one is the vanishing of positive ion density at the wall to all orders) to the diffusion layer equation, which is of second order. Solving the diffusion layer problem gives the ϵ -order change of number density gradient at the wall.

From reference 3, the first approximation to a blunt subsonic probe is accurate to within 10% without correction, due to the cancellation between the compressibility and heat transfer corrections. This is because in general, the change of diffusivity at the wall prevails over the change of number density gradient there. The effect of compressibility is to decrease the diffusion coefficient near the wall, and thus to decrease the current collected. The effect of a hotter wall (the probe is hotter than the environment) is to increase the diffusion coefficient near the wall, and thus to increase the current collected.

IV Experiments

From Section II, it is obvious that measurements by supersonic probes can be highly inaccurate. Section III then supplied the theoretical basis for the operation of a blunt subsonic probe. It is on this basis that seven Arcas meteorological rockets have been launched, of which six night

launches were particularly successful, with the data showing close repeatability between 50 and 60 km. The launch site was White Sands, N. M.

The first two launches (one being a Sirocco rocket) were made at daytime in September and December 1964, which showed periodic oscillations having an amplitude of about 10% of the total current. It was found out that the frequency of those oscillations coincide with the pendulum frequency of the parachute-probe system. This angle of attack dependence in turn could be attributed to the photo-electric control of the probe system. This was borne out by nighttime launches on and after 21 March 1965, which showed little or no angle of attack dependence, and current proportional to probe potential. Having thus verified Hoult's first order probe theory, Hale⁽⁵⁾ measured the positive and negative conductivity profiles, computed the ion density profiles using assumed values of ion mobility and CIRA atmosphere model and checked these profiles with results from his chemistry model (equation 3) using the CIRA model as well. These two approaches give very close agreement in the range of 50-63 km.

To see how the variation of the angle of attack affects the current collected during daytime, let us first examine the division of potentials of a symmetric bipolar probe. During daytime, $\lambda \ll \mu^e / \mu^+$ in the range of consideration, so the current to a positive electrode will be the electron current. Comparing (7) and (8), noting that the two electrode areas are about the same, the electric field of the negative electrode, and hence the voltage there, must have a much larger absolute value than that of the positive probe, approaching a ratio of μ^e / μ^+ when $\lambda \leq 1$. In fact a low impedance connection is provided between the positive probe and the space.

Solar radiation in the 2000-3000 Å range penetrates down to the ozone layer, which can produce photo-electric current to drastically alter

the situation discussed above. There will be a net electron flow from the more negative probe to the less negative probe. When this photo current is high enough, more so when the angle of attack increases and thus raising the lumen of the probe system, it may prevail over the environmental effect. Furthermore, there is a net loss of electrons from the probe system. Hence in actual descent the negative electrode is getting closer and closer to the space potential, or may even become positive. Table 1 of reference 4 clearly shows this tendency, which is based on accepted values of photo-electric currents.

The division of applied potential between the current collector and the return electrode during nighttime is very different from that during daytime. This different mechanism is utilized to good advantage by constructing asymmetric probes in the last two experiments, which consisted of silvered parachutes and silvered shroud lines, thus greatly increasing the area of the return electrodes. At night, $\lambda \gg \mu^e / \mu^-$ is satisfied in the lower D-region, then (8) becomes

$$dI_o^- \approx \sigma_{\infty}^- E_w ds$$

Noting that the applied sweep potential $V_A = |V_P - V_R|$ (Subscripts P and R denote probe and return electrode respectively), with the above equation and (7), we obtain (neglecting the shroud line current)

$$\begin{aligned} |V_P^-| &= \frac{V_A}{1 + \frac{\sigma_{\infty}^+ L_P}{\sigma_{\infty}^- L_R}} = \frac{V_A}{1 + \alpha \gamma} \\ V_P^+ &= \frac{V_A}{1 + \frac{\sigma_{\infty}^- L_P}{\sigma_{\infty}^+ L_R}} = \frac{V_A}{1 + \frac{\gamma}{\alpha}} \end{aligned} \quad (9)$$

where:

$$L_P = \frac{1}{V_P} \int_P E_w ds$$

$$L_R = \frac{1}{V_R} \int_R E_w ds$$

$$\alpha = \frac{\sigma_{\infty}^+}{\sigma_{\infty}^-}$$

$$\gamma = \frac{L_P}{L_R}$$

In the case of an asymmetric probe, the two electrodes are far apart by insulation⁽⁵⁾, consequently L_P and L_R are proportional to the free space self capacitances of the geometries employed, with γ roughly equal to $S_P/S_R \ll 1$. In fact there is a low impedance connection between the return electrode and the space by virtue of the large electrode surface. Within the sweep range of V_A , V_P practically takes up all the voltage applied, with V_R virtually short-circuited with the space. For two electrodes in close proximity, such as the bipolar case, γ tends to unity⁽⁵⁾.

For a small collector, the electric field at the collector wall is (reference 2)

$$E_w = \frac{V}{\pi R}$$

where V and R are probe voltage and probe radius respectively. Using the above equation and (9), we can rewrite (7) as

$$I_O^+ = \sigma_{\infty}^+ \frac{r^2}{R} V_A \frac{1}{1 + \alpha \gamma} \quad (10)$$

Similarly for the negative ion current towards a positive collector

$$I_O^- = \sigma_{\infty}^- \frac{r^2}{R} V_A \frac{1}{1 + \frac{\gamma}{\alpha}} \quad (11)$$

In the case of an asymmetric probe, the current ratio in two different modes of operation

$$I_o^+ / I_o^- = \sigma_{\infty}^+ / \sigma_{\infty}^-$$

In the case of a symmetric probe, $\gamma \cong 1$, for the first four night launches

$$I_o^+ = I_o^- = \frac{r^2}{R} V_A \left(\frac{\sigma_{\infty}^+ \sigma_{\infty}^-}{\sigma_{\infty}^+ + \sigma_{\infty}^-} \right)_{\infty}$$

Hence with an asymmetric probe we can now distinguish the positive conductivity from the negative conductivity, an improvement over the earlier symmetric probes. The sweep voltage and telemetered current waveforms are shown in fig. 4⁽⁵⁾, from which it is evident that the linear relation between the probe voltage and current holds; the blunt probe is insensitive to the variation of angle of attack; and that it is possible to separate negative and positive conductivities with an asymmetric probe. The measured ion conductivities of six launches are plotted in fig. 5 of reference 5. From fig. 5, a closely repeatable plot, it is shown that the negative conductivity exceeds the positive conductivity by about 25% below 63 km, in close agreement to accepted ratios of mobilities of small ions (molecular weight about 30). This prompted Hale to use about the same ratio for mobilities, basing his argument on the small ion model.

Assuming values of positive ($1.8 \text{ cm}^2/\text{volt-sec}$) and negative ($2.3 \text{ cm}^2/\text{volt-sec}$) ion mobilities at a reference altitude, using the assumption that μ^i is proportional to $\frac{T^i}{\rho}$, along with the average CIRA model atmosphere, Hale computed the ion density profile from the conductivity measurements, which are plotted in fig. 6 of his paper⁽⁵⁾. Then using a galactic cosmic ray ionization rate of $0.075/\text{cm}^3\text{-sec}$ at 60 km and

the CIRA model, Hale plotted the ion density profile from his simplified chemistry model as described by (3), which is also included in fig. 6 for comparison. They agree very well in the range of 50-63 km, giving the α_i value (assumed to be constant within that range) around $3.3 \times 10^{-3} \text{ cm}^3/\text{sec}$, and the λ value in excess of a thousand below 63 km. Daytime ion density profile for the first two launches is computed likewise save the uncertainties in probe potential due to photo-electric effects. This is shown in fig. 4 of reference 4. The ion density profile above 63 km is discussed in reference 5.

V Conclusions

(1) The sweep voltage and telemetered current waveforms indicate a linear relationship between current and probe voltage and the insensitivity of the blunt probe to the variation of the angle of attack, thus verifying Hoult's theory.

(2) Negative conductivity exceeds positive conductivity by around 25% from 50 km to 63 km during nighttime. This distinction between positive and negative conductivities is realized using Hale's concept on asymmetric probes.

(3) Hale's chemistry model for nighttime lower D region seems to agree with his conductivity measurements. The uncertainty, among others, rests on the assumption of ionic mobilities in data reduction.

References

1. Hoult, D. P., "Weak Shock Waves in the Ionosphere", J. Geophys. Res., 69, 4617-4620 (1964).
2. Hoult, D. P., "D-Region Probe Theory", J. Geophys. Res., 70, 3183-3187 (1965).
3. Hoult, D. P. and T. J. Kuo, "First-Order Corrections to D-Region Probe Theory", J. Geophys. Res., 71, 3191-3200 (1966).
4. Hale, L. C., Hoult, D. P. and Willis, R. G., "Preliminary Results of Rocket Measurements of D-Region Ion Density", Electron Density Profiles in the Ionosphere and Exosphere, 108, North Holland Publishing Co., 1966.
5. Hale, L. C., "Parameters of the Low Ionosphere at Night Deduced from Parachute Borne Blunt Probe Measurements", Proceedings of Seventh International Space Science Symposium, Vienna, Austria, May 1966.
6. Reid, G. C., "Physical Processes in the D Region of the Ionosphere", Rev. of Geophysics, Vol. 2, 2, 311-333 (1964).

Acknowledgments

I wish to thank Dr. D. P. Hoult for guidance and criticism of the work, to Dr. L. C. Hale for helpful discussions and to the staff of the Ionosphere Research Laboratory, Pennsylvania State University.